Comparative Measurements of WLS Fibers

M. David, A. Gomes, A. Maio
LIP and Univ. of Lisbon, Lisbon, Portugal
A. Henriques
CERN, Geneva, Switzerland
Y. Protopopov
IHEP, Serphukhov, Russia
D. Jankowski, R. Stanek
Argonne National Laboratory, USA

Abstract

The optical properties of several types of polystyrene WLS fibers are compared. Fibers having different dopant and UV absorber concentrations, and with different claddings have been measured. Experimental results on the light yield, light transmission, and mechanical stress tolerance of these fibers are presented. A comparative study of those properties is done for Kuraray, Bicron and Pol.Hi.Tech fibers.

1 Introduction

A comparative study of the optical properties of different polystyrene WaveLength Shifter (WLS) fibers produced by Kuraray, Bicron and Pol.Hi.Tech have been performed in order to optimize the performance of the TILECAL/ATLAS calorimeter. Systematic measurements of the fiber light output and transmission have been done as a function of several parameters and under different physical conditions, such as:

- Dopant concentration
- UV absorber concentration
- Fiber cladding
- Mechanical stress

The proposed ATLAS hadronic calorimeter for the barrel and extended barrel regions will use scintillating polystyrene tiles and WLS plastic fibers to collect and transmit light from the plastic scintillators to the photomultipliers (PMT's). In some cases the light must travel down the fibers for more than one meter and fibers with good attenuation lengths as well as high light yield are necessary. We have looked at the light yield as a function of the dopant concentration, as well as cladding type. Fibers from different manufacturers have been tested. Table 1 lists the various types of fibers measured and their specific characteristics.

Furthermore, it has been shown in prior test beam results with either muons or pions impinging on the crack region between scintillators, that there is an enhancement of the calorimeter response by about a factor of 1.5 [1]. This extra enhancement leads to nonuniformity across the calorimeter and should be minimized. It is known that charged particles hitting WLS bars [2] or WLS fibers [3] generate Cerenkov and/or scintillation light. So to reduce this effect in the crack region of TILECAL we have investigated the addition of small concentrations of UV absorber (UVA) to the mixture used in commercial standard fibers.

Although not being a serious problem for the TILECAL calorimeter, the degradation of optical transmissivity over time is a concern if the fibers are stressed by bending. To understand these factors we have measured the transmission through WLS fibers with varying degrees of stress.

In section 2 we give a brief description of the setups used and the measurement procedures. Section 3.1 presents results on the integrated current measurements for fibers illuminated either with a blue scintillator or excited directly with a β-source. Section 3.2 compares absolute numbers of photoelectrons measured for fibers excited with β particles and for scintillator illuminated fibers. Section 4 presents results on light degradation of fibers under mechanical stress. Finally in section 5 we present a summary of the results.

2 Experimental setup

2.1 Current measurement

Fibers are excited at different distances (x) from an EMI9813KB bi-alkali photocathode photomultiplier using light from a TILECAL blue scintillator, which is excited by electrons from a ^{90}Sr β-source. The scintillator/β-source system moves along each fiber. In some of the measurements only the β-source itself was used to excite the light directly in the fiber. One precise way of comparing the relative light emission and light transmission is done by integrating the PMT current $I(x)$. The PMT signal is read by a digital voltmeter and data acquisition is made by a Macintosh equipped with a GPIB interface [4]. The position of the excitation source along the fiber is obtained from a stepping motor controller. The system was equipped with LABVIEW

software.

A reference fiber sitting in a fixed position inside the box is used to monitor the stability of these measurements. We estimate systematic errors of $\lesssim$2.5% [4] with a 2% (sigma) error on the light yield I_0, and about 6% for the attenuation length.

The Bicron and Pol.Hi.Tech fibers measured in this setup are 200 cm long and Kuraray fibers are 150 cm long. All fibers were polished at the end close to the PMT and the opposite end was painted black. Three fibers of each type have been measured. Figure 1 shows the light output as a function of the distance to the PMT for three BCF91A fibers. Fiber to fiber fluctuations were found to be of the order of 5% in the light output for each group of 3 (or 4) fibers.

2.2 Number of photoelectron measurements

The system for measuring the absolute number of photoelectrons N_{pe} has been described elsewhere [5] but will be summarized here. 3 MeV electrons are selected from a ^{106}Ru source by a spectrometer. The electrons from the ^{106}Ru source are required to excite a pair of trigger scintilators, thus ensuring the selection of a MIP. Samples of fibers or scintillator are taped to a plate perpendicular to the electron beam. This plate is precisely translated in either the vertical (y) or the horizontal (x) plane by means of a computer controlled stepping motor.

Light output from scintillator samples are coupled through fibers to a Hammamatsu R580 phototube. When scanning fibers, these fibers are directly coupled to the phototube. The contact to the PMT is through optical grease. The output of the R580 is digitized, gated by the scintillator coincidence, and the ADC distribution is recorded for 2000 triggers per (x,y) coordinate.

We estimate the source width to be about 1.5 - 2 mm FWHM. Systematic error associated with the manipulation of the fibers at the PMT is estimated at around 5%.

A set of fibers placed in the y direction were driven past the β-source, illuminated at 50 cm from the PMT in order to measure the direct (Cerenkov and/or scintillation) light yield in the fibers. The ADC distributions were recorded as a function of the illumination position (x).

The light output along the length of the fiber was measured in a similar way as described above but using the scintillation light to illuminate the fibers. The ADC distribution was measured as the fiber contact point to the scintillator was varied from 30 cm to 90 cm with 10 cm steps.

All fibers for the N_{pe} measurements were 100 cm long, also blackened on the far end.

3 Comparative results

We compare the response to the scintillator light from some typical fibers from Bicron, Kuraray and Pol.Hi.Tech in Fig. 2. In this figure we plot the light output $I(x)$ of the fibers as a function of the distance x from the excitation point to the PMT. These values can be fitted with the sum of two exponentials as follows:

$$I(x) = I_{01} \exp\left(-\frac{x}{L_1}\right) + I_{02} \exp\left(-\frac{x}{L_2}\right) \quad (1)$$

L_1 - Short attenuation length (in cm).
L_2 - Long attenuation length (in cm).
$I_{01} + I_{02}$ - Light yield at $x = 0$ cm.

All the data were fitted with Eq. 1 and the light yield and attenuation length parameters are used for comparison purposes.

Figure 3 shows the ratio of the signal for each typical fiber type normalized to the BCF91A fiber as a function of x. Figure 4 shows the signal output at x=140 cm for each typical fiber type normalized to the BCF91A fiber at the same x.

3.1 Light yield and transmission. Current measurements.

3.1.1 Effect of the dopant concentration

In this section we present the effect of dopant concentration in the light yield and light transmission of the fibers. The scintillator light was used to illuminate the fibers. For this purpose we have studied several types of fibers:

- BCF91A (concentration 1x), BCF-99-28 (conc. 2x) and BCF-99-36 (conc. 4x) from Bicron.
- S048-2-100 (conc. 2y), S048-3-100 (conc. 3y), S048-4-100 (conc. 4y) and S048-6-100 (conc. 6y) from Pol.Hi.Tech.
- Y7, Y8, Y9, Y10 and Y11 from Kuraray. For these fibers dopant concentration is given in ppm (inside brackets).

Bicron and Pol.Hi.Tech fibers used in this concentration effect study come from a special production for this purpose. In table 2 and Figs. 5, 6 and 7 experimental and fit results are presented. We observe that the light yield extrapolated by the fit to x=0 cm ($I_{0T} = I_{01} + I_{02}$), increases slightly with the dopant concentration

for Bicron and Kuraray fibers, while the Pol.Hi.Tech fibers show a strong increase with a maximum yield about 4y for the extrapolated light yield and this maximum is already reached for 3y at x=140 cm. For the Y7 fibers this maximum is obtained for concentrations $>$ 250 ppm.

Referring to table 2 for clarity, we point out several features. For almost all the fibers, the short attenuation length L_1 decreases with increasing dopant concentration. The long attenuation length L_2 for the Bicron fibers remains approximately constant (240 cm), but for Pol.Hi.Tech fibers L_2 decreases from 290 cm to 135 cm when concentration increases from 2y to 6y . For Y11 and Y7 fibers both L_1 and L_2 decrease with increasing concentration.

Comparing the light output of all fibers at x=50 cm and x=140 cm it is seen that increasing the dopant concentration does not necessarily lead to an increase in light output at all values of x even though I_{0T} increases with increasing dopant. This is simply an effect of Eq. 1 where the light output is a product of the attenuation and the local yield. This point is most dramatic for the S048 fibers where we see a peak light output at the 3y concentration at x=95 and 140 cm. Similarly, for Y11 fibers the decrease in attenuation length is masked by the increase in light yield when the dopant concentration increases. The yield at 250 ppm is about the same as for 400 ppm, even though I_{0T} increases. For the Y7 fibers a saturation is visible for dopant concentrations $>$ 150 ppm at $x \geqslant 50$ cm.

For any fiber type, a compromise between light yield and attenuation length as function of dopant concentration should be settled. Further studies with smaller UVA concentrations, with other types of double clad fibers under development by the manufacturers, and with PMT's similar to the ones to be used in TILECAL are envisaged.

3.1.2 Effect of the UV absorber concentration

As in section 3.1.1, Bicron fibers with different percentages of UVA were measured using excitation light from the scintillator to study the effect of this parameter in the light yield and light transmission. The light output $I(x)$ is shown in Fig. 8.

Experimental and fit results are summarized in table 3. The short (L_1) and the long (L_2) attenuation lengths decrease when the concentration of UVA increases, especially L_2, which goes from 227 cm to 88 cm with the addition of 2.0% of UVA. The total light yield I_{0T} stays roughly the same for all fibers, but as discussed above, due to the strong decrease in attenuation length, $I(x)$ at $x > 50$ cm decreases when UVA concentration increases.

We observed that the WLS fibers with polystyrene base produce light when excited with a radioactive source and, as mentioned before, with high energy e^-, π^- and μ beams. This light could come from the Cerenkov light produced inside the fibers subsequently shifted to the emission spectra of the fibers, or scintillation light coming

from the polystyrene base. To study the direct light output produced by charged particles, the scintillator was removed from the setup and the fibers were excited directly with electrons from the ^{90}Sr β-source.

Experimental and fit results are shown in table 4. Fig. 9 and table 4 shows the direct light output for the several Bicron fibers with different UVA concentrations. From Fig. 9 we can see that to supress the effect of light produced directly by charged particles a concentration smaller than 0.06% can be used. Those results show that there is still place for a better compromise between high light output and good uniformity on the tile/fiber system.

3.1.3 Effect of the cladding

Most of the fibers tested have a single PMMA cladding. Kuraray also produces fibers with fluorinated PMMA cladding and double clad fibers. The 1 mm double clad fibers consist of a fiber core 880 micron diameter, an inner cladding and an outer cladding, both 30 micron thick [6].

From the results presented in Figs. 2, 3 and 4 it is shown that for the Kuraray fibers a factor of 1.25 in light output at 140 cm is obtained when comparing double and single clad Y11(200) fibers. From those results it is also shown that a factor of 1.30 in light output at 140 cm can be achieved when the response of Y11(200)MS fibers is compared with the response of Bicron fibers.

Since the several fibers under tests do not necessarily have the same spectral light output and different PMT's are used in bench tests, systematic measurements have been performed using phototubes with different spectral quantum efficiency. Besides the EMI9813KB "blue" PMT used in the tests reported above, typical fibers have also been tested with the green extended Philips XP2081B and with the Philips XP2012 used also in the TILECAL prototype. The spectral quantum efficiency of the PMT foreseen to be used in ATLAS is somewhere between that of the EMI9813KB and the XP2081B. In table 5 we present a summary of these comparisons for $x \simeq 40$ and 140 cm. The values in the table are light outputs normalized to the response of the standard BCF91A fibers. For fibers Y11(200)MS at x=140 cm a factor of 1.30 is obtained for the EMI9813KB while a factor of 1.6 is obtained when an XP2012 is used. This result was clearly confirmed in test beam with the TILECAL prototype [7].

3.2 Light yield and transmission. Number of photoelectrons measurements

Photoelectron yield is calculated in the following manner. First the ADC is calibrated with an LED generating a relatively large amount of light. The number of photoelectrons (N_{pe}) from the LED can then be calculated from the mean and width of the ADC spectrum:

$$N_{pe} = (\frac{< ADC >}{\sigma})^2 \quad (2)$$

We now know the calibration constant between mean ADC channel and N_{pe}. For our samples, the mean ADC channel is calculated using *all* the ADC channels, including zero. It is this mean channel times the calibration constant which is used to calculate the N_{pe} yield. Note that the calibration done for a region of relatively large amount of light is extrapolated for the region of small number of photoelectrons (N_{pe} <1).

3.2.1 Fiber response to electrons

Figure 10 shows typical responses from the fibers as a function of the source position across them.

The data from each fiber is fit to a gaussian as shown. The widths of all these curves are fairly constant, and the mean σ is 0.85 mm which is consistent with the width of the β-source. Since the zeros in the ADC distribution can come from both inefficiency in the fiber as well as triggers where the electron does not pass through the fiber, we need to correct the measured photoelectron yield for the width of the beam. From the measured width of 0.85 mm, a correction factor of 2.7 is calculated and applied to the uncorrected values.

3.2.2 Effect of the dopant concentration

For the light output of fibers excited by scintillator light, we can parametrize the photoelectron yield with Eq. 1. The light yield using this parametrization is shown in Fig. 11 as a function of dopant concentration. Those results show that there is only a weak dependance of the light yield on dopant content for the Bicron, while the Pol.Hi.Tech fibers show a maximum yield at about 3-4y, in agreement with the current measurements described in section 3.1.1.

In Fig. 12 it is shown, for fibers excited by MIP's, the photoelectron yield as a function of dopant concentration for Bicron and Pol.Hi.Tech. The trend for Bicron shows an increasing light yield as the dopant is increased, while the trend for Pol.Hi.Tech shows a maximum at about 3y concentration. A summary of the photoelectron yields for the various conditions discussed above are given in tables 6 - 7. Similar results are obtained with the current measurements, see Figs. 5, 6 and 7 and table 2.

Those results show that the slight increase of light output with the dopant concentration is followed by an increase in direct response to MIP's. For calorimeter purposes not only lhe level of light output is important but also the non uniformity across the calorimeter. The choice of the dopant concentration should take into account the ratio between the fiber response to scintillator light and to MIP's.

3.2.3 Effect of the UV absorber concentration

Figure 13-top and table 8 show the light output measurements at 50 cm from the PMT as a function of UVA concentration for the Bicron fibers excited by MIP's. Those results should be compared with the current measurements (Fig. 13-bottom), presented also in Fig. 9 and table 4. We see that the addition of the slightest amount (0.06%) of UVA quenches the direct light, and that the addition of higher concentrations has little additional effect.

In Fig. 14 and table 9 are presented the light output measurements for Bicron fibers excited by the tilecal scintillator. Those results should also be compared with current measurements (Fig. 8 and table 3).

Although the direct light is dramatically reduced as the UVA concentration increases, the light induced by the scintillator is reduced only by about 20% with the addition of a small amount of UVA, both for the near light component, as well as the far light component.

Those results show that it is still possible to reduce significantly the direct light by using UVA concentrations less than 0.06%. A compromise between low production of direct light and high intensity of the light induced by the scintillator should be achieved.

The summary of the results presented in sections 3.2.2 and 3.2.3 is shown in Fig. 15.

4 Stress resistance

A decrease of attenuation length due to micro-cracks of plastic fibers under stress is a cause of fiber ageing. We investigate the ageing as a function of the stress from bending fibers at different radii.

We parametrize the fragility of the fibers as the ratio of attenuation lengths for 45 cm long fibers after stressing to before stressing, $L_r = L_{post-stress}/L_{pre-stress}$. Fibers were bent with diameters of 5, 7.5, 10, 15, 20 cm and kept in this state for 100 hours. After this time period the light output was again measured with the fiber straight.

Typical behaviour of the fibers is shown in Fig. 16. The relative light attenuation length L_r for Y7 and BCF99-28A is shown as a function of the bending diameter. In the diameter range 10-15 cm an intensive cracking of Y7 starts which leads to a fast decrease of the attenuation length. The diameter 16 mm corresponds to the physical breaking point of a Y7 fiber. For BCF99-28A fibers the breaking diameter D_{break} is smaller than 1 mm. These results indicate a relationship between fragility and D_{break}, thus giving an opportunity to estimate fiber fragility by measuring its breaking diameter.

D_{break} for the different types of WLS fibers are given in table 10. Light output of 3 types of WLS fibers at a distance 40 cm from PMT after stress is shown in table 11. These results show that Bicron fibers can be bent without damage up to very small radii, and the same is valid for RK-27 fibers produced by INR, as well as for Kuraray 'S' type fibers.

We know from Kuraray that 'S' type means that a little different condition of fiber drawing is used to improve the mechanical strength under bending. In fact the example shown in table 10 of Y11(200)MS ilustrates this characteristic. Some of the Pol.Hi.Tech fibers show also promising mechanical stress properties.

5 Summary

A comparative study of the optical properties of Bicron, Pol.Hi.Tech and Kuraray WLS fibers have been performed as a function of several parameters. The experimental results are summarized as follows:

- The light yield increases with the dopant concentration at the expense of some decrease in the attenuation length. The optimal concentration for Bicron fibers is about 3x, for S048 fibers it is about 4y, and for Kuraray Y11 it is less than 250 ppm.

- The light produced by WLS fibers when excited with ionizing radiation is not negligible, leading to non-uniformities in the calorimeter. This effect can be strongly reduced using an UV absorber.

  Direct light induced by ionizing radiation is strongly reduced as the UVA concentration increases, while light induced by the scintillator is reduced very slightly (about 20%). Optimization is still possible using UVA concentration less than 0.06%.

- Double cladding Y11(200) fibers from Kuraray present the highest light output for scintillator-PMT distances greater than 100 cm. A factor of 1.6 is obtained when compared with the response of BCF91A fibers using an XP2012 PMT.

- Some of the Pol.Hi.Tech fibers show promising mechanical properties. Fragility of Bicron and Kuraray 'S' type fibers are acceptable for the TILECAL calorimeter.

References

[1] TILECAL internal comunications

[2] K.Z. and O.Gildmeister, Cerenkov Light Absorption by a UV-absorber in Calorimeter Wavelength Shifter Plates (for the central calorimeter of UA2 experiment), $p\overline{p}$ note 106, 1980

[3] A. Benvenuti et al., Prototype design, construction and test of a Pb/scintillator sampling calorimeter with wavelength shifter fiber optic readout, IEEE Transactions on Nuclear Science, Vol. 40, No. 4, 1993

[4] B. Tome et al, Test bench for quality control of scintillating and WLS fibers, LIP note 5-10-94

[5] D. Jankowski and R. Stanek, Response of ATLAS Injection Molded Scintillators, TILECAL-No-010

[6] B. Baumbaugh et al., Performace of multiclad scintillating and clear waveguide fibers read out with visible light photon counters, NIM A345 (1994) 271-278
A. Byon-Wagner, Recent Developments in Scintillating tile and WLS fiber for the SDC Calorimeter, ICFA Instrumentation Bulletin No. 9, 1993
SDC Technical Proposal, SDC-92-201

[7] A. Ariztizabal et al., Construction and Performance of an Iron-Scintillator Hadron Calorimeter with Longitudinal Tile Configuration, NIM A349 (1994) 384-397

Company	Fiber type	Concent. of dopant	Concent. of UV absorber	Type of cladding
Bicron	BCF-91A	1x	-	Single
	BCF-99-28	2x	-	Single
	BCF-99-36	4x	-	Single
	BCF-99-28XA	2x	0.06%	Single
	BCF-99-28XB	2x	0.25%	Single
	BCF-99-28XC	2x	1.00%	Single
	BCF-99-28XD	2x	2.00%	Single
Pol.Hi.Tec.	S048-100	?	-	Single
	S048-2-100	2y	-	Single
	S048-3-100	3y	-	Single
	S048-4-100	4y	-	Single
	S048-6-100	6y	-	Single
	S049-2-100	2y	-	Single
	S053-2-100	2y	-	Single
	S054-2-100	2y	-	Single
Kuraray	Y7(60)	60	-	Single
	Y7(100)	100	-	Single
	Y7(150)	150	-	Single
	Y7(150)N	150	-	Single,fl.PMMA
	Y7(250)	250	-	Single
	Y8(100)	100	-	Single
	Y8(150)	150	-	Single
	Y8(250)	250	-	Single
	Y9(30)	30	-	Single
	Y9(50)	50	-	Single
	Y9(100)	100	-	Single
	Y10(50)	50	-	Single
	Y10(100)	100	-	Single
	Y10(200)	200	-	Single
	Y11(100)M-S-type	100	-	Double
	Y11(200)S-type	200	-	Single
	Y11(200)M-S-type	200	-	Double
	Y11(250)	250	-	Single
	Y11(400)	400	-	Single

Table 1: **Specification of the several types of fibers**.
x is the nominal concentration of dopant given by Bicron.
y is the nominal concentration of dopant given by Pol.Hi.Tec.
For Kuraray fibers the dopant concentration is given in p.p.m.

Fiber type	Dopant conc.	L_1 (cm)	L_2 (cm)	I_{0T}	I(50 cm)	I(95 cm)	I(140 cm)
BCF91A	1x	19.3	242	2.18	1.07	0.82	0.69
BCF-99-28	2x	15.7	227	2.40	1.00	0.78	0.64
BCF-99-36	4x	14.4	247	2.49	1.03	0.83	0.70
S048-2-100	2y	16.7	290	0.86	0.45	0.36	0.32
S048-3-100	3y	16.6	281	1.50	0.74	0.62	0.53
S048-4-100	4y	15.8	169	1.72	0.77	0.58	0.46
S048-6-100	6y	16.2	135	1.69	0.61	0.39	0.29
Y11(250)	250	14.3	217	2.43	1.06	0.83	0.69
Y11(400)	400	12.7	211	2.56	1.04	0.81	0.68
Y7(60)	60	21.6	235	1.11	0.58	0.46	0.37
Y7(100)	100	20.9	195	1.40	0.67	0.51	0.39
Y7(150)	150	20.2	188	1.69	0.79	0.59	0.45
Y7(250)	250	18.2	168	1.95	0.79	0.58	0.43
				I_{6cm}			
Y8(100)	100			0.62	0.32	0.25	0.20
Y8(150)	150			0.74	0.40	0.31	0.25
Y8(250)	250			0.93	0.52	0.36	0.28
Y9(30)	30			1.06	0.55	0.41	0.31
Y9(50)	50			1.39	0.69	0.47	0.32
Y9(100)	100			1.69	0.67	0.41	0.24
Y10(50)	50			1.37	0.72	0.52	0.39
Y10(100)	100			1.62	0.76	0.53	0.36
Y10(200)	200			1.73	0.69	0.43	0.27

Table 2: **Light output for fibers with different concentrations of dopant. Fibers were illuminated with scintillator light.** L_1 and L_2 are the short and the long attenuation lengths respectively, taken from equation 1. I_{0T} is the light yield at x=0 cm taken from the fit. I(50 cm), I(95 cm) and I(140 cm) are the measured light outputs at 50, 95 and 140 cm from the PMT, respectively.

Fiber type	Fiber #	UVA conc.	L_1 (cm)	L_2 (cm)	I_{0T}	I (50 cm)	I (95 cm)	I (140 cm)
BCF-99-28	1	0%	15.1	226	2.43	1.01	0.75	0.65
BCF-99-28	2	0%	15.9	221	2.41	1.02	0.81	0.65
BCF-99-28	3	0%	16.0	236	2.36	0.98	0.76	0.64
Average			**15.7**	**227**	**2.40**	**1.00**	**0.78**	**0.64**
BCF-99-28XA	1	0.06%	14.2	159	2.27	0.81	0.58	0.44
BCF-99-28XA	2	0.06%	19.7	173	1.99	0.76	0.53	0.41
BCF-99-28XA	3	0.06%	12.5	153	2.59	0.90	0.65	0.48
Average			**15.5**	**161**	**2.28**	**0.83**	**0.59**	**0.44**
BCF-99-28XB	1	0.25%	14.0	135	2.42	0.89	0.62	0.44
BCF-99-28XB	2	0.25%	12.7	132	2.52	0.90	0.62	0.44
BCF-99-28XB	3	0.25%	16.1	139	2.24	0.91	0.63	0.45
Average			**14.3**	**135**	**2.39**	**0.90**	**0.62**	**0.44**
BCF-99-28XC	1	1.00%	13.2	108	2.21	0.71	0.45	0.31
BCF-99-28XC	2	1.00%	13.7	115	2.43	0.81	0.53	0.37
BCF-99-28XC	3	1.00%	14.3	100	2.06	0.70	0.41	0.27
Average			**13.7**	**108**	**2.23**	**0.74**	**0.46**	**0.32**
BCF-99-28XD	1	2.00%	11.4	85	2.35	0.68	0.39	0.24
BCF-99-28XD	2	2.00%	12.7	91	2.36	0.72	0.42	0.26
BCF-99-28XD	3	2.00%	10.9	87	2.66	0.73	0.43	0.27
Average			**11.7**	**88**	**2.46**	**0.71**	**0.41**	**0.26**

Table 3: **Light output for fibers with different concentration of UV absorber. Fibers were illuminated with light from a Tilecal scintillator.** L_1 and L_2 are the short and the long attenuation lengths respectively, taken from equation 1, I_{0T} is the light yield at x=0 cm taken from the fit, I (50 cm), I (95 cm) and I (140 cm) are the measured light outputs at 50, 95 and 140 cm from the PMT.

Fiber type	UVA conc.	L_1 (cm)	L_2 (cm)	I_{0T}	I (50 cm)	I (95 cm)	I (140cm)
BCF-99-28	0%	15.1	249	2.78	1.22	0.96	0.82
BCF-99-28XA	0.06%	14.1	207	0.66	0.25	0.19	0.16
BCF-99-28XB	0.25%	11.3	180	0.55	0.19	0.15	0.12
BCF-99-28XC	1.00%	10.2	162	0.49	0.13	0.10	0.08
BCF-99-28XD	2.00%	10.4	120	0.42	0.12	0.08	0.06

Table 4: **Light output (Cerenkov or scintillating) for fibers with different concentration of UV absorber illuminated with electrons from a ^{90}Sr β-source.** L_1 and L_2 are the short and the long attenuation length respectively, taken from equation 1, I_{0T} is the light yield at x=0 cm taken from the fit, I(50 cm), I(95 cm) and I(140 cm) are the measured light outputs at 50, 95 and 140 cm from the PMT.

PMT	XP2012		XP2081B	EMI9813KB			
x (cm)	140	140	140	45	40	140	140
Ref.	1	2	3	4	5	6	7
Fiber							
BCF91A	1	1	1	1	1	1	1
S048-100	-	-	0.94	-	0.91	-	0.96
Y11(200)MS	1.6	1.6	1.51	-	1.14	-	1.30
Y11(200)S	1.2	-	-	1.04	0.92	1.02	1.07
Y11(100)MS	1.4	-	-	0.94		1.03	
Y11(100)S	1.2	-	-	0.90	-	0.93	-
Y7(150)N	1.1	-	-	0.71	-	0.61	-
Y7(150)	0.9	-	-	0.74	-	0.63	-

Table 5: **Summary of light output for several fibers, for typical distances and for several photomultipliers. All values are relative to BCF91A fibers.** Ref. 1- one pair of fibers. Ref. 2- Test beam results. Ref. 3- two pairs of fibers. Refs. 4,6- 1.5 m long fibers, neither black painted nor polished at the side opposite to the PMT. Refs. 5,7- 2.2 m long fibers, also polished at the side opposite to PMT.

Fiber type	Conc. dopant	I (50 cm)	I (95 cm)	N_{pe} (50 cm)	N_{pe} (90 cm)
BCF91A	1x	1.06	0.82	0.77	0.55
BCF-99-28	2x	1.01	0.78	0.75	0.52
BCF-99-36	4x	1.03	0.83	0.82	0.59
S048-2-100	2y	0.43	0.36	0.28	0.13
S048-3-100	3y	0.74	0.62	0.34	0.19
S048-4-100	4y	0.77	0.58	0.57	0.12
S048-6-100	6y	0.60	0.39	0.13	0.08

Table 6: **Light output for fibers with different concentrations of dopant. Fibers were illuminated with scintillator light.** N_{pe} (50 cm) and N_{pe} (90 cm) are the photoelectron yields measured at 50 and 90 cm from the PMT. For comparison, the measured currents I (50 cm) and I (95 cm) at 50 and 95 cm are also given.

Fiber type	Conc. dopant	$N_{pe_{MAX}}$ (50 cm)
BCF91A	1x	0.38
BCF-99-28	2x	0.46
BCF-99-36	4x	0.57
S048-2-100	2y	0.19
S048-3-100	3y	0.35
S048-4-100	4y	0.30
S048-6-100	6y	0.19

Table 7: **Light output (Cerenkov or scintillating) for fibers with different concentration of dopant illuminated with electrons from a ^{90}Sr β-source.** $N_{pe_{MAX}}$ (50 cm) is the peak photoelectron yield measured at 50 cm from the PMT.

Fiber type	UV absor. concent.	I (50 cm)	$N_{pe_{MAX}}$ (50 cm)
BCF-99-28	0%	1.22	0.46
BCF-99-28XA	0.06%	0.25	0.14
BCF-99-28XB	0.25%	0.19	0.05
BCF-99-28XC	1.00%	0.13	0.08
BCF-99-28XD	2.00%	0.12	0.03

Table 8: **Light output (Cerenkov or scintillating) for fibers with different concentration of UV absorber illuminated with electrons from a ^{90}Sr β-source.** I (50 cm) and $N_{pe_{MAX}}$ (50 cm) are the relative current and peak photolectron yield measured at 50 cm from the PMT.

Fiber type	Conc. UV absor.	I (50 cm)	I (95 cm)	N_{pe} (50 cm)	N_{pe}(90 cm)
BCF-99-28	0%	1.01	0.78	0.75	0.52
BCF-99-28XA	0.06%	0.81	0.59	0.73	0.41
BCF-99-28XB	0.25%	0.89	0.62	0.52	0.35
BCF-99-28XC	1.00%	0.71	0.46	0.61	0.38
BCF-99-28XD	2.00%	0.68	0.41	0.51	0.28

Table 9: **Light output for fibers with different concentrations of UVA. Fibers were illuminated with scintillator light.** N_{pe} (50 cm) and N_{pe} (90 cm) are the photolectron yields measured at 50 and 90 cm from the PMT. For comparison, the measured current I (50 cm) and I (95 cm) at 50 and 95 cm is also given.

Fiber type	D break (mm)
BCF-91A	< 1
BCF-99-36	3
BCF-99-28	< 1
BCF-99-28XA	< 1
BCF-99-28XB	< 1
BCF-99-28XC	3
BCF-99-28XD	< 1
S048-2-100	16
S048-3-100	11
S048-4-100	10
S048-6-100	6
S049-2-100	18
S053-2-100	10
S054-2-100	2
Y11(200)M-S-type	< 1
Y7(100)	16
Y7(180)M	12
Y8(150)	18
Y11(200)	12

Table 10: **Breaking diameter for several fiber types.**

Fiber type	D curvature (mm)	relative light output in the distance 40 cm from PMT, %
Y7(100)	200	100
	150	98
	100	32
	75	20
	50	12
BCF-99-28A	200	100
	150	100
	100	100
	75	99
	50	97
RK-27 (INR, Moscow)	200	100
	50	100
	42	97

Table 11: **Mechanical stress.** Variation of light output with curvature diameter.

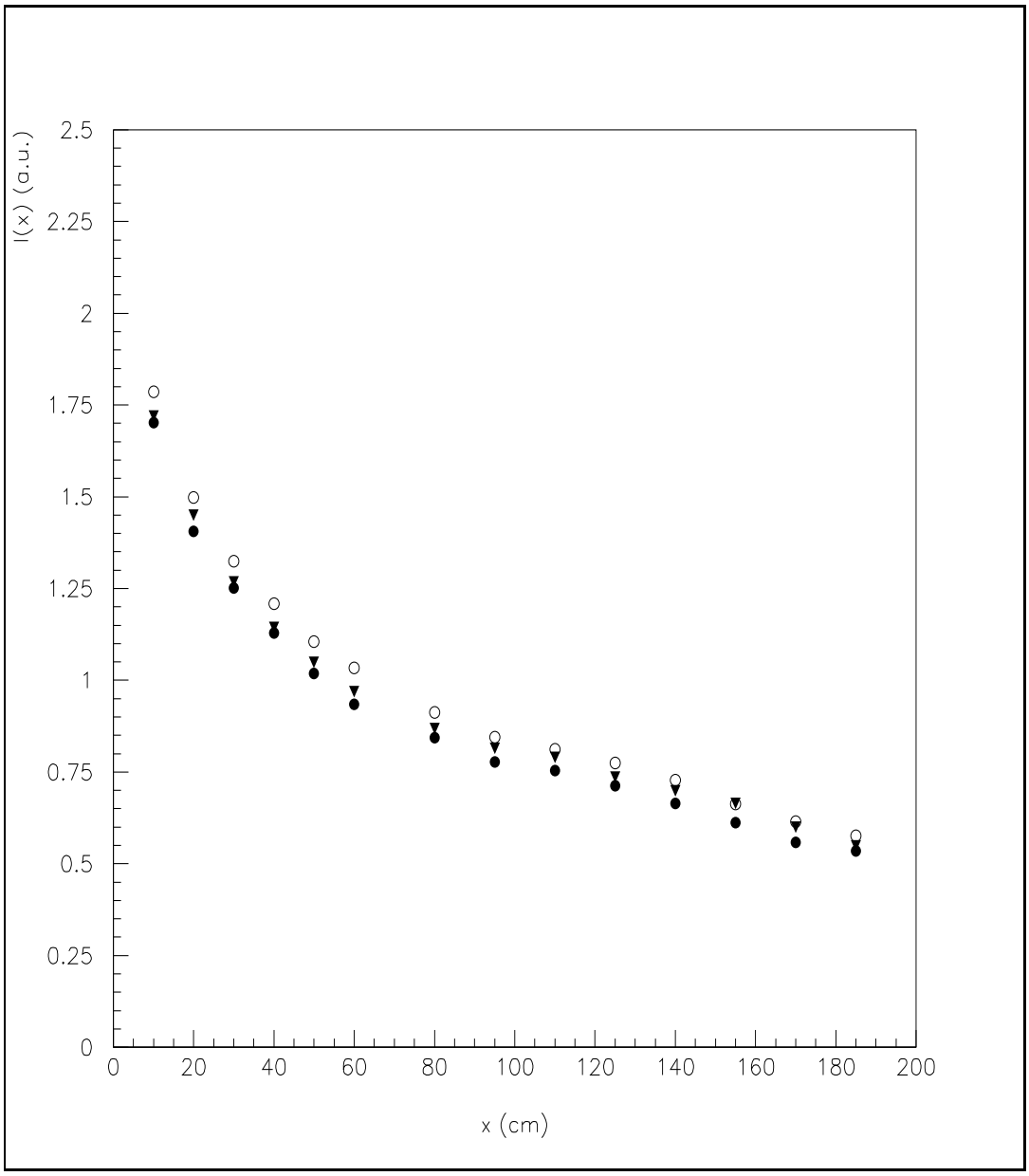

Figure 1: Light output of 3 BCF91A fibers as function of the distance x of excitation point to the PMT. Fibers illuminated with TILECAL scintillator light.

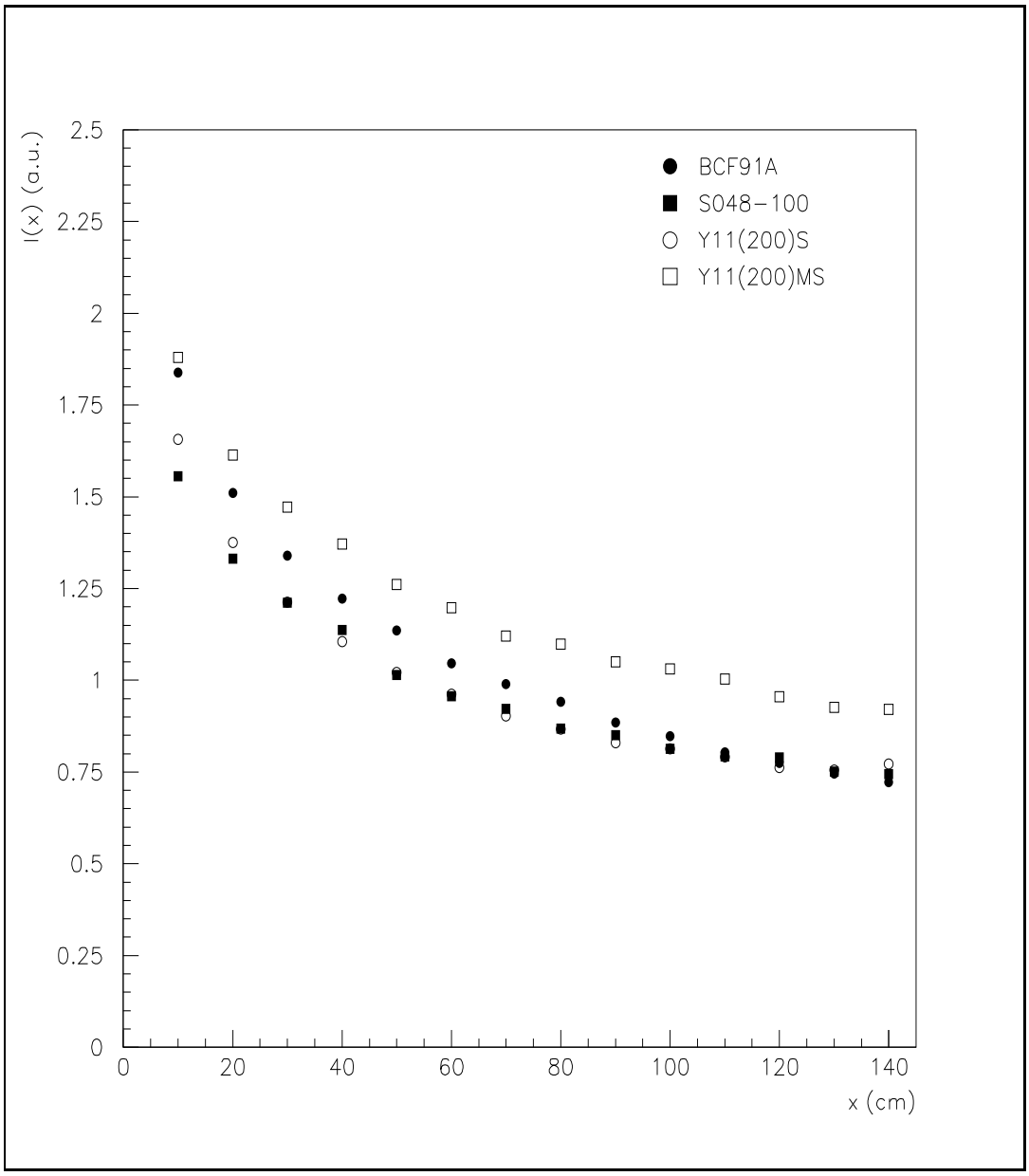

Figure 2: Light output for some typical fibers from Bicron, Kuraray and Pol.Hi.Tech. Fibers illuminated with TILECAL scintillator light.

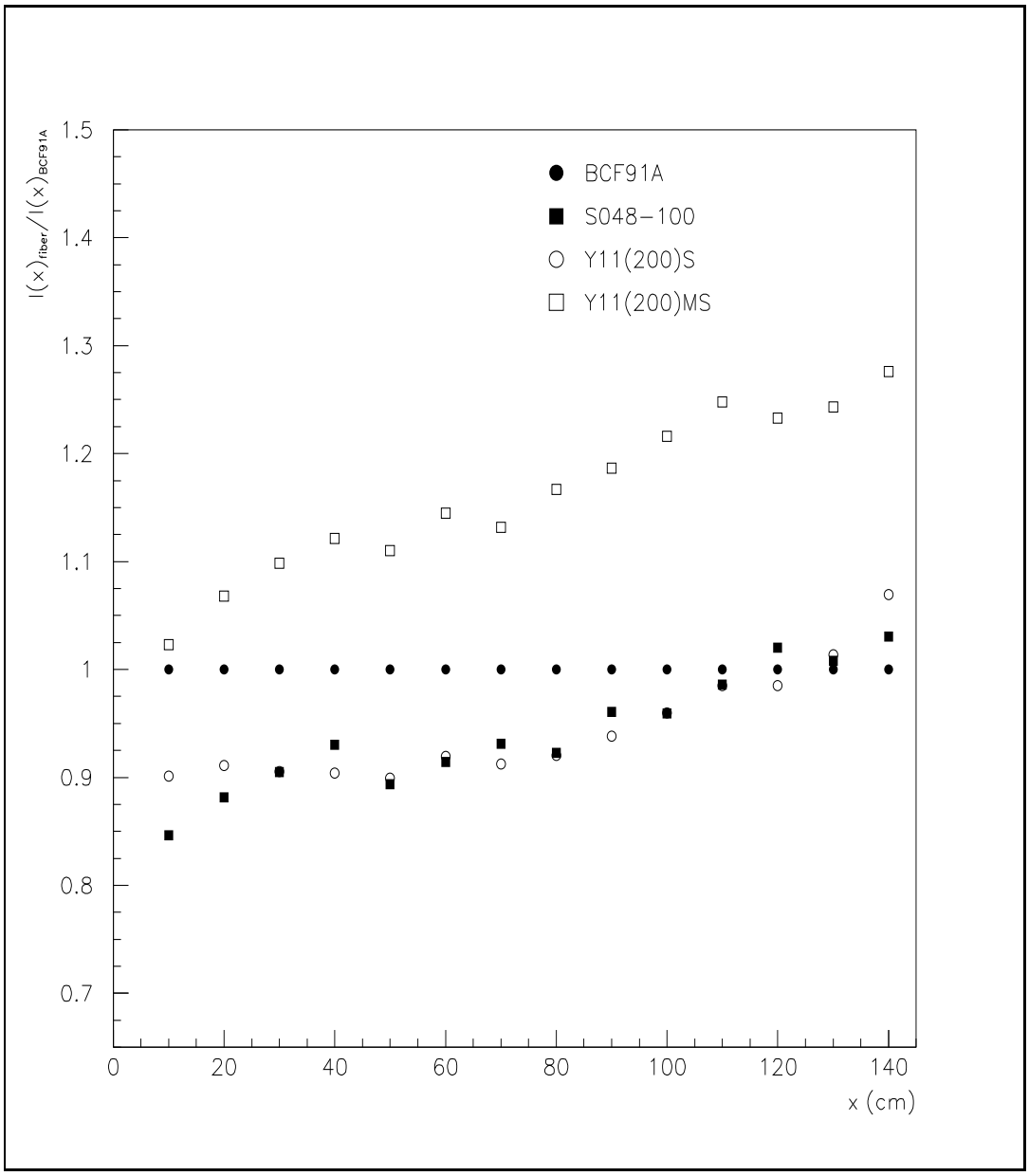

Figure 3: Typical fibers. Light output is normalized to the BCF91A fiber for each distance. Fibers illuminated with TILECAL scintillator light.

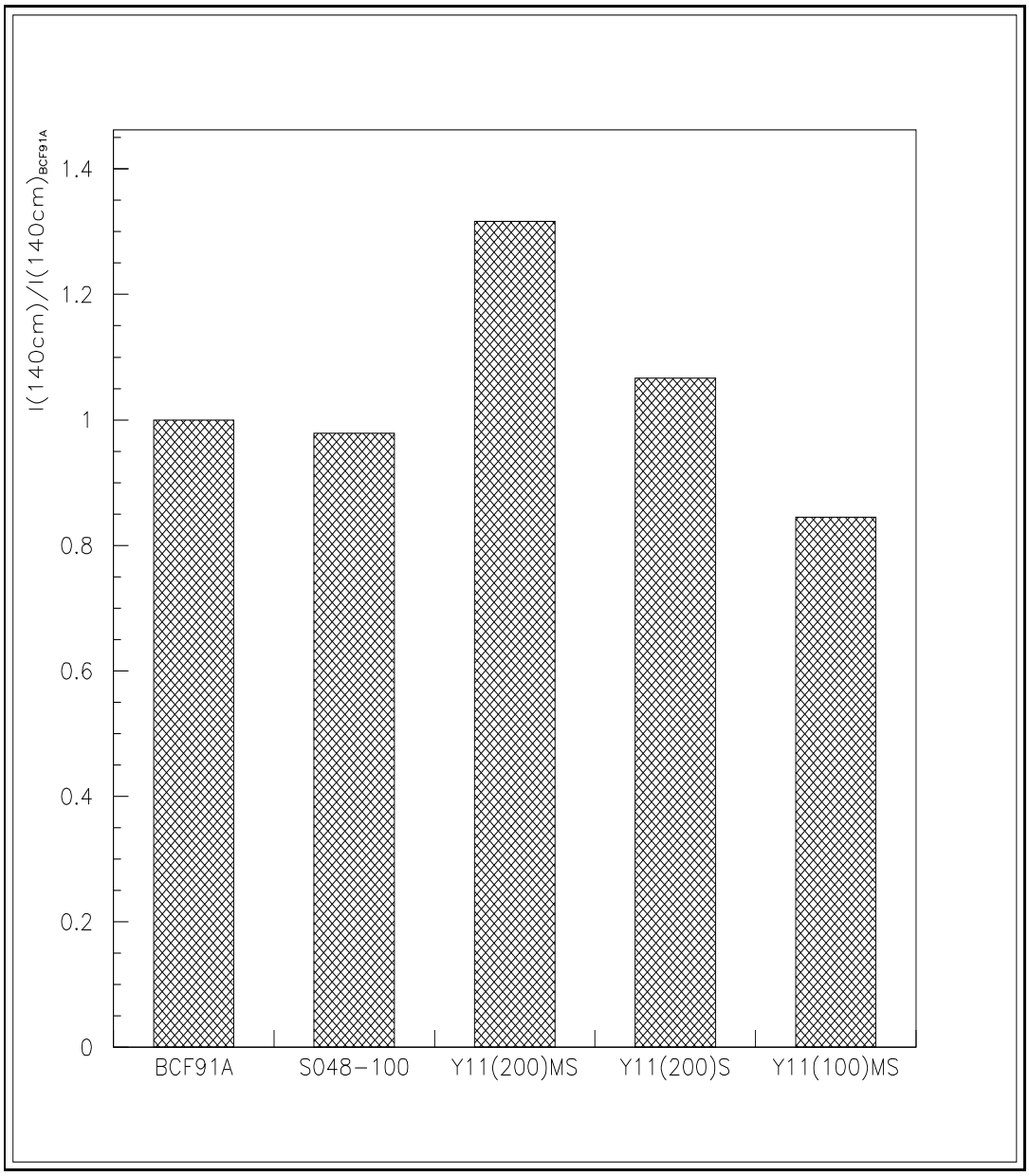

Figure 4: Light output at x=140 cm for some typical fibers (normalized to BCF91A). Fibers illuminated with TILECAL scintillator light.

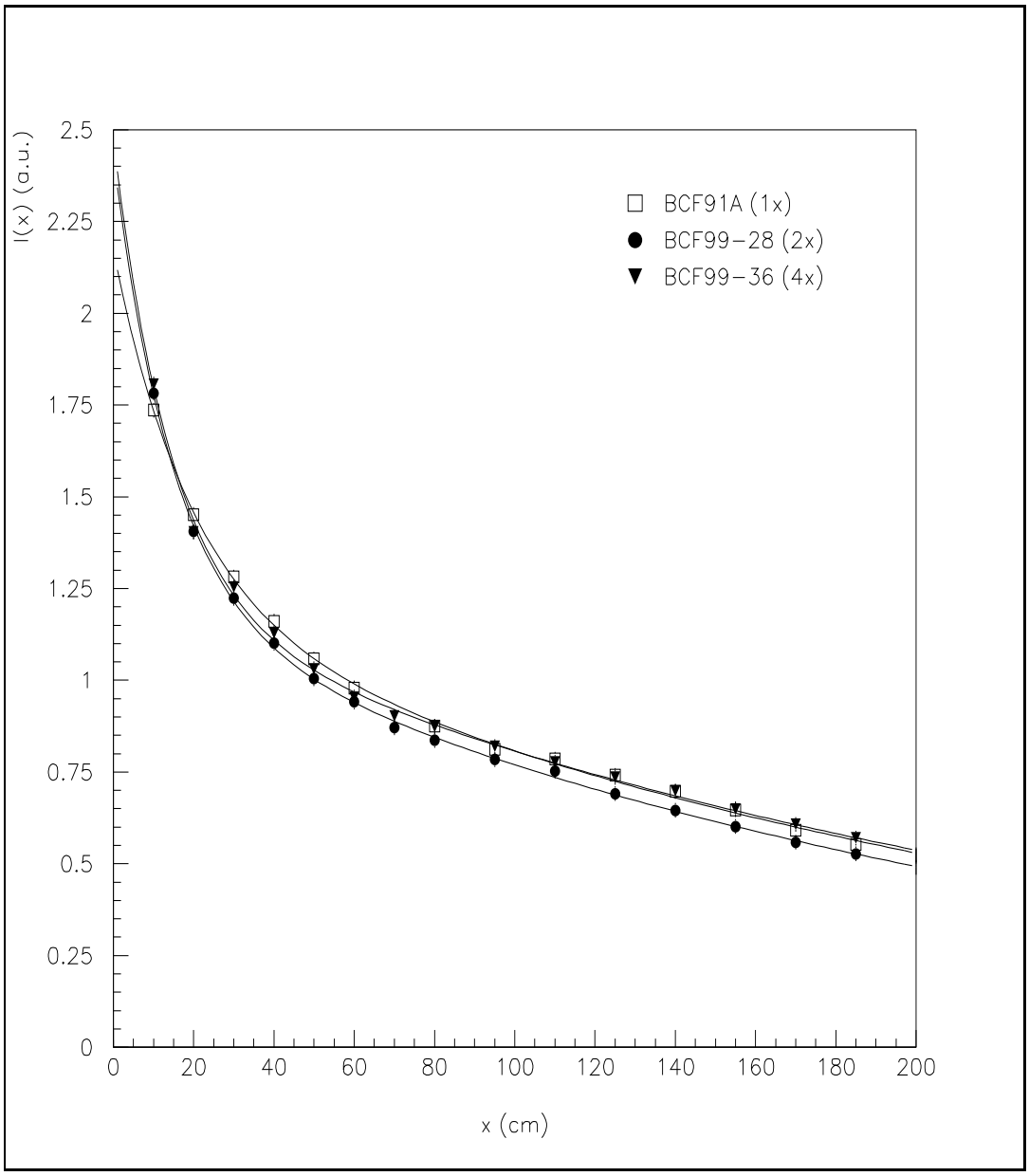

Figure 5: Light output for Bicron fibers with different dopant concentrations. Fibers illuminated with TILECAL scintillator light.

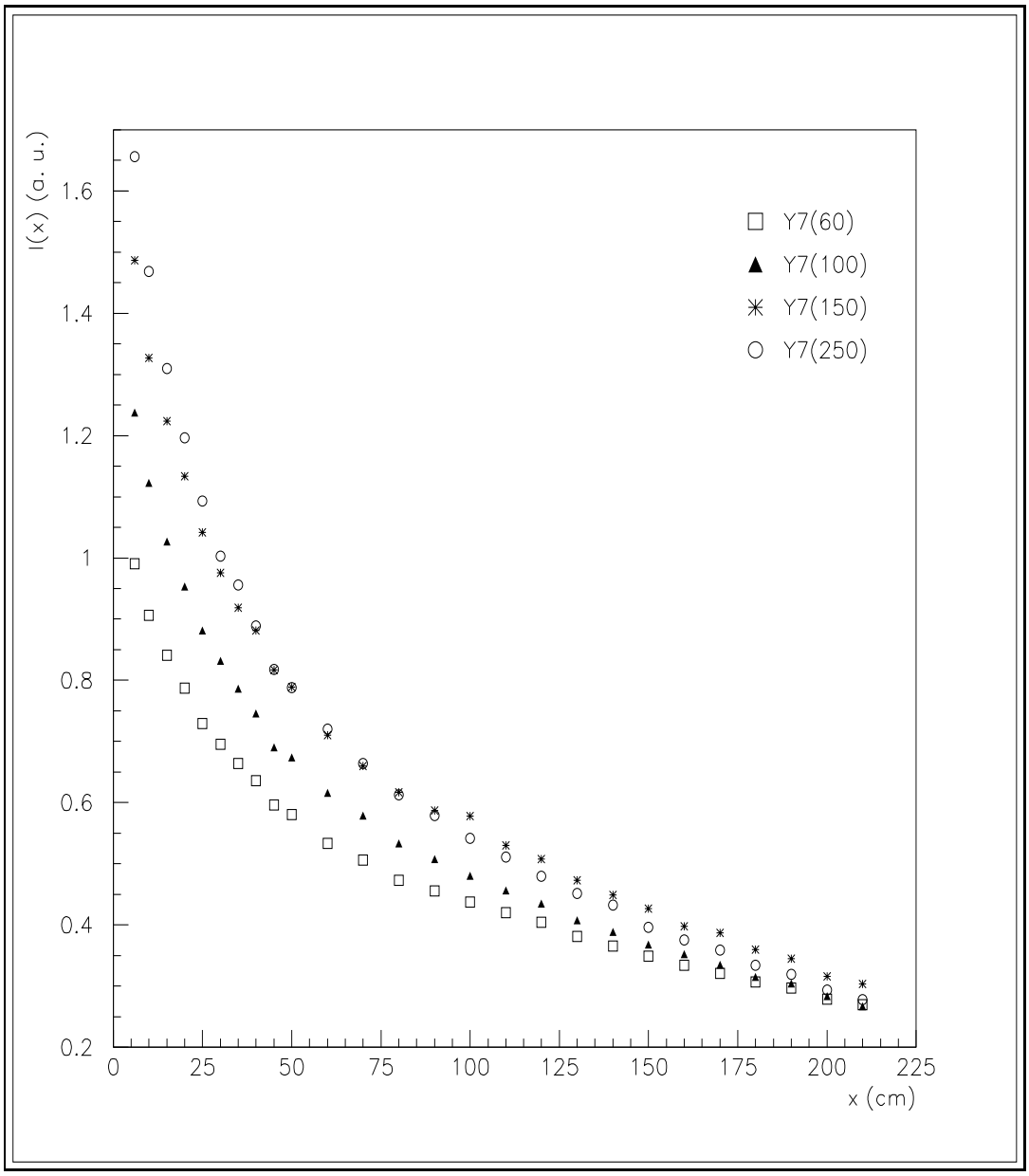

Figure 6: Light output for Y7 fibers with different dopant concentrations. Fibers illuminated with TILECAL scintillator light.

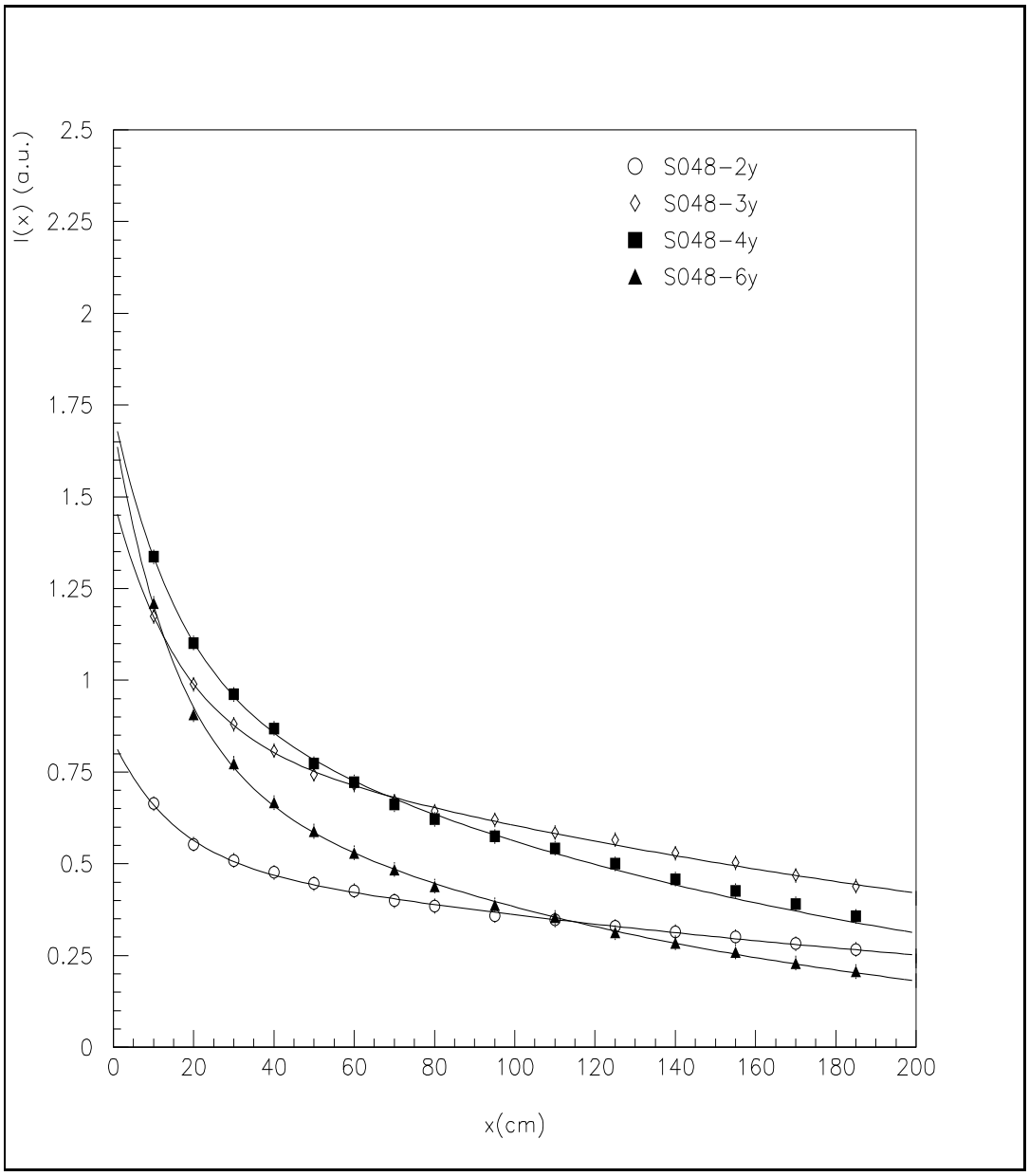

Figure 7: Light output for Pol.Hi.Tech fibers with different dopant concentrations. Fibers illuminated with TILECAL scintillator light.

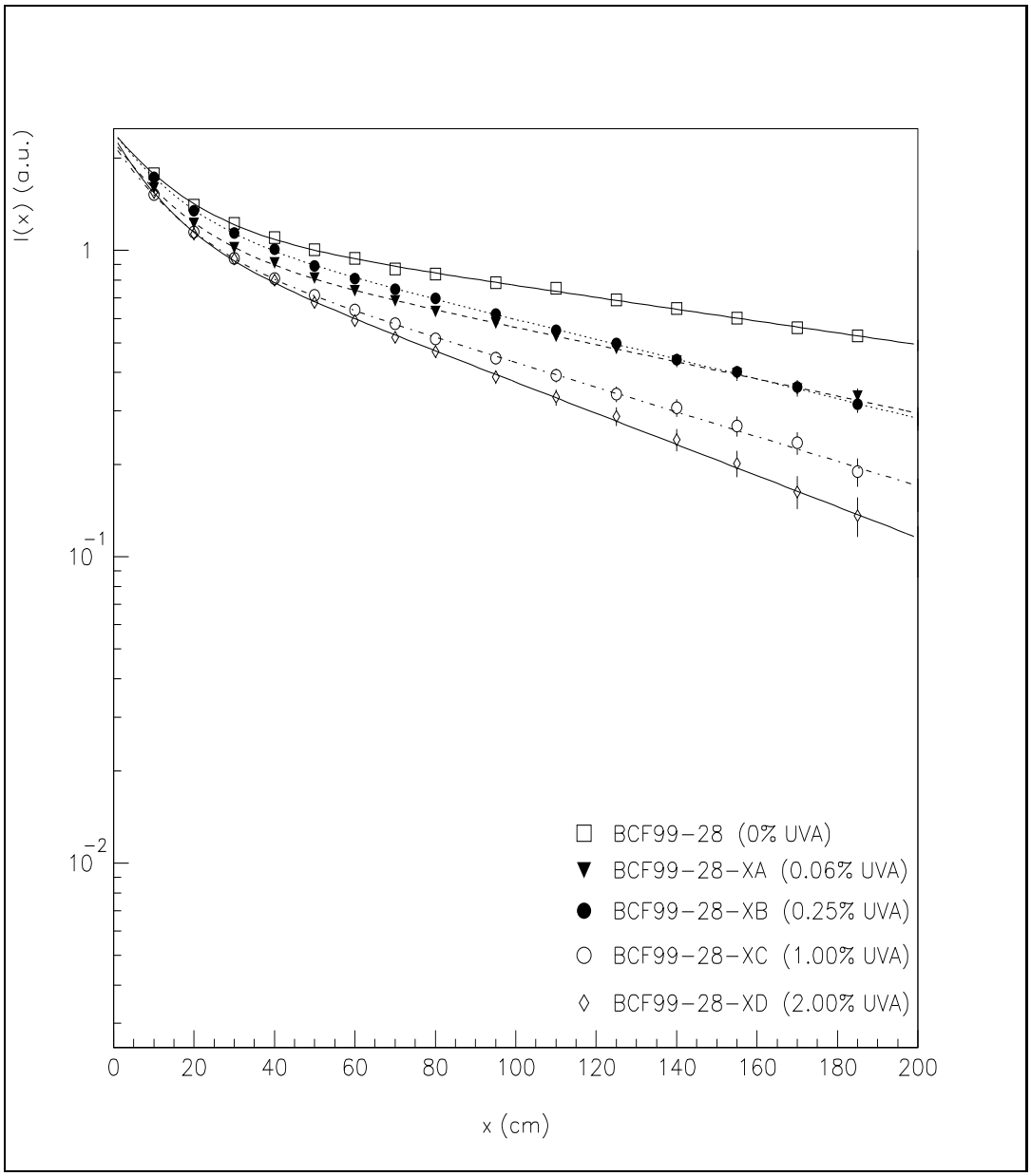

Figure 8: Light output for Bicron fibers with different UVA concentrations. Fibers illuminated with TILECAL scintillator.

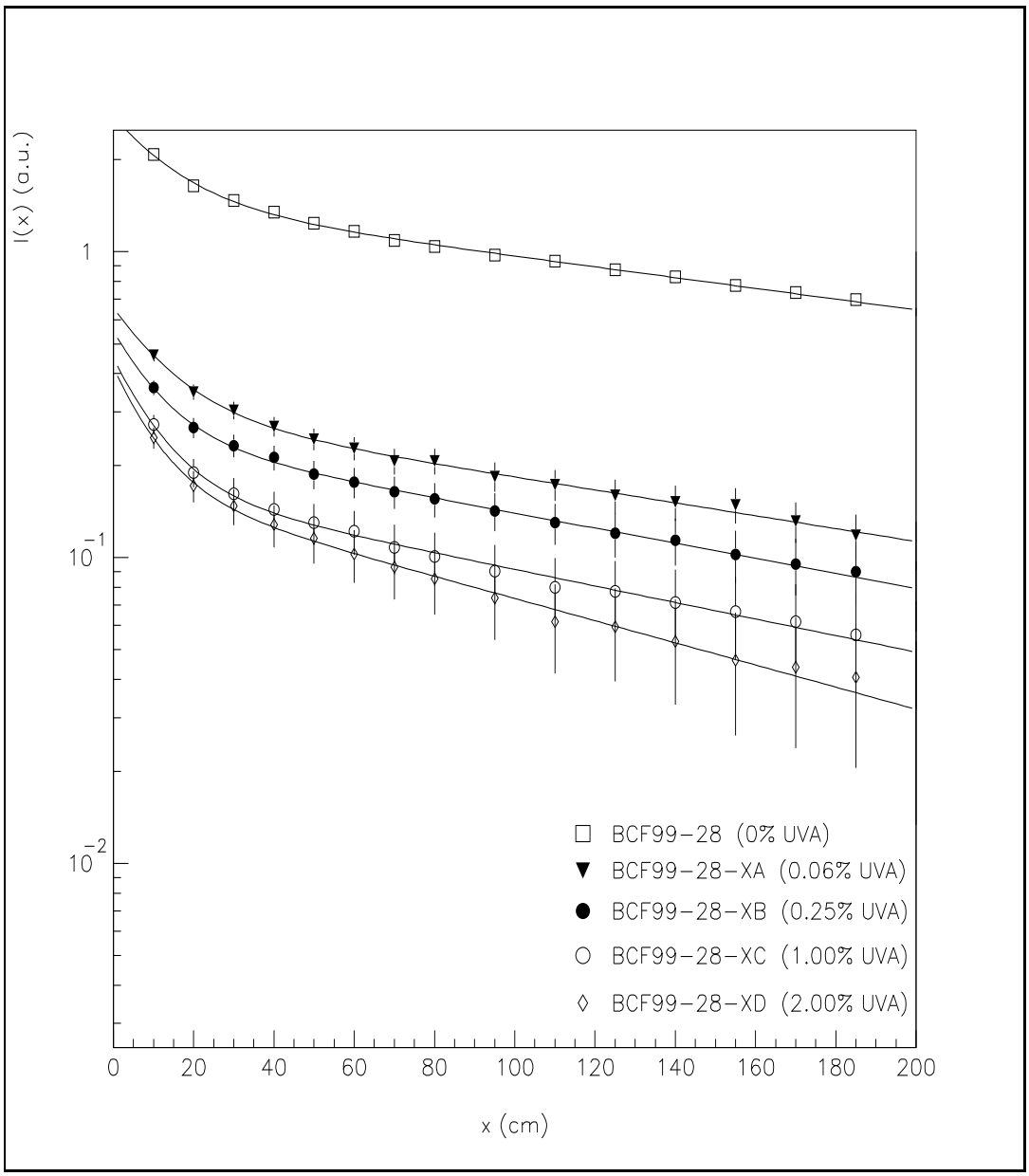

Figure 9: Light output (Cerenkov or scintillating) for Bicron fibers with different concentrations of UV absorber. Fibers illuminated with electrons from a ^{90}Sr β-source.

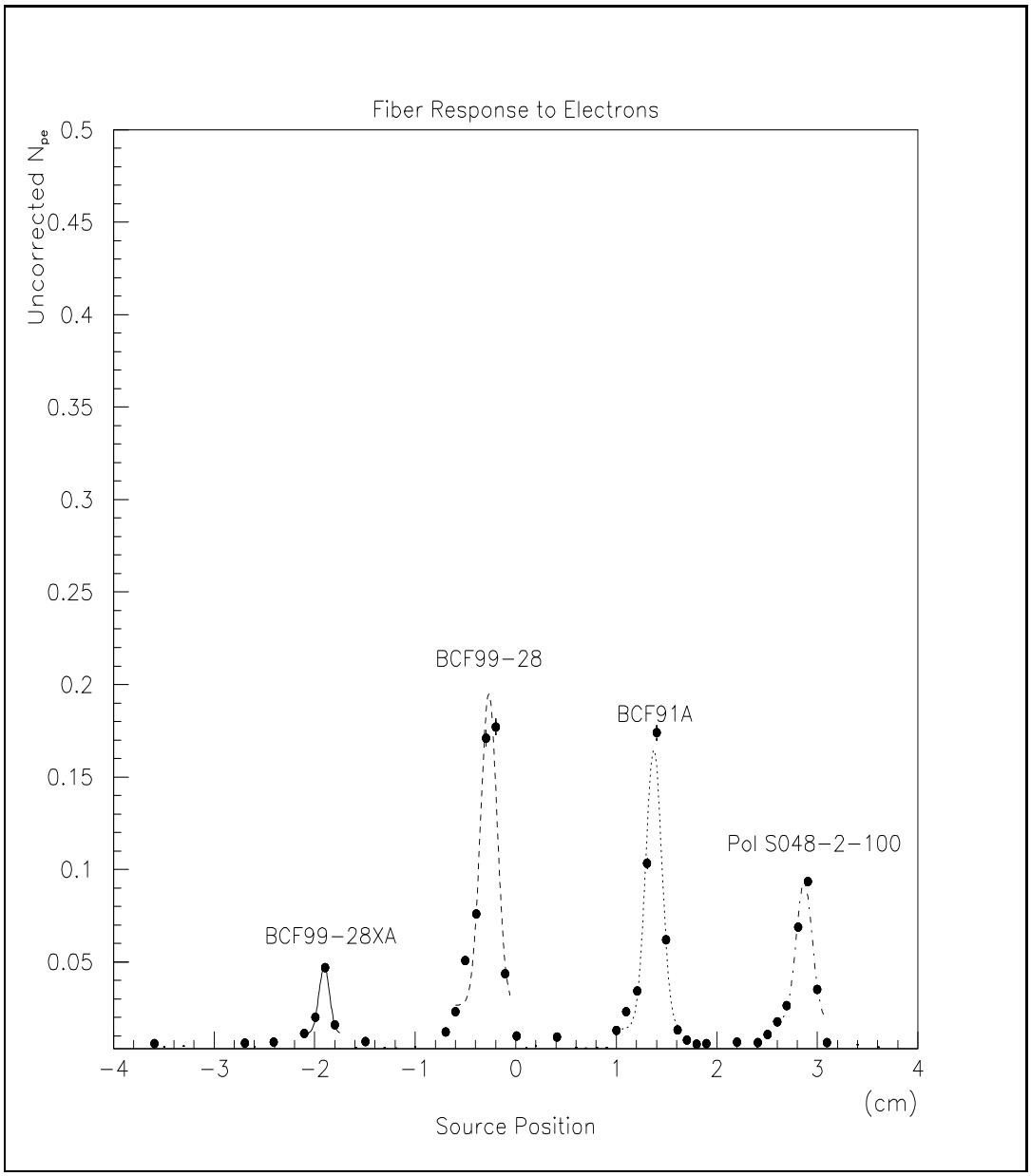

Figure 10: Typical fiber photoelectron yield to a MIP. The photoelectron yield is not corrected for the width of the β-source. Fibers illuminated with electrons from a ^{106}Ru β-source.

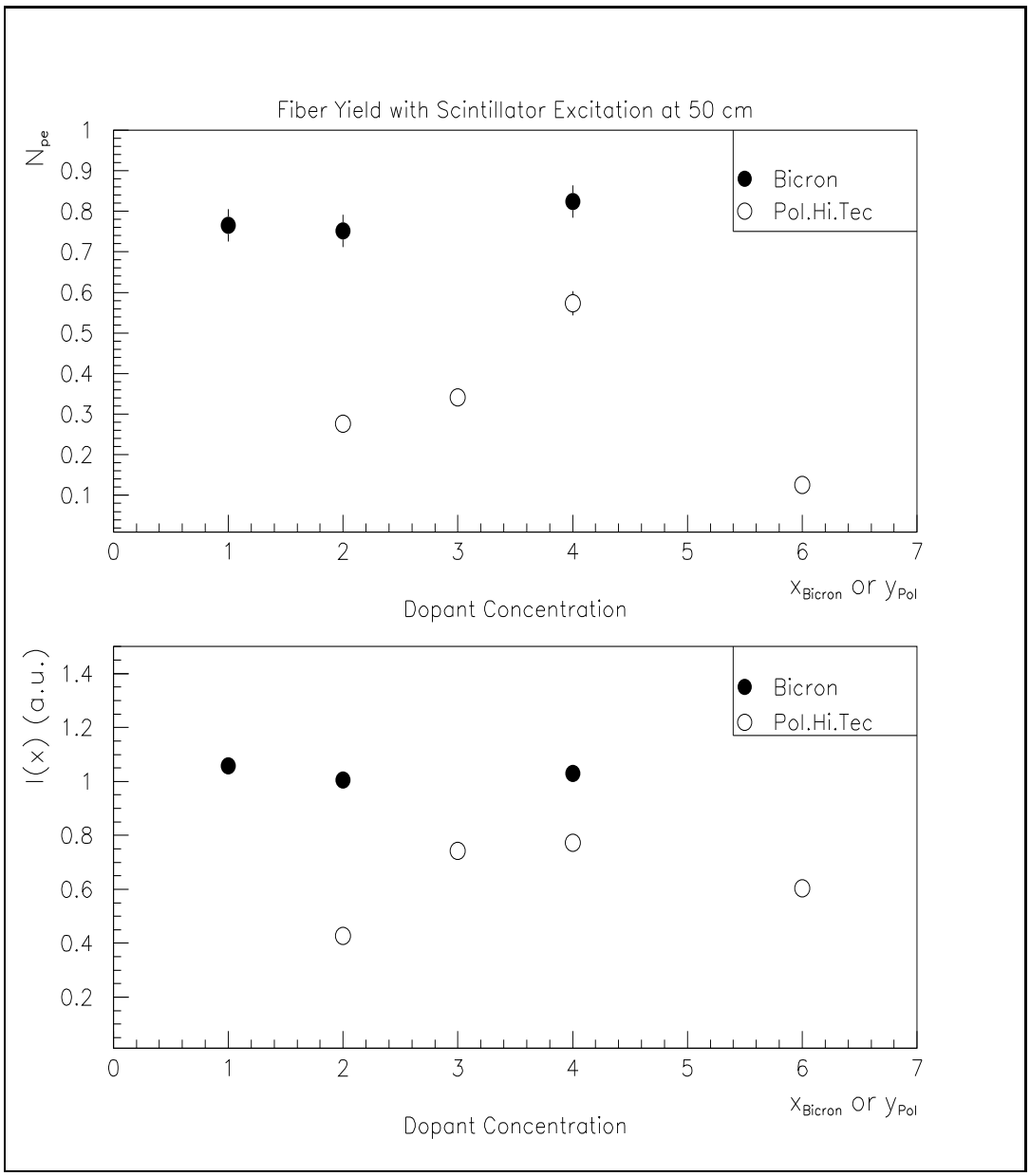

Figure 11: Light yields for fibers with varying concentrations of dopant. x is the standard Bicron concentration, and y is the standard Pol.Hi.Tech concentration. The top figure shows the photolectron yield measured for Bicron and Pol.Hi.Tech with the scintillator at 50 cm from the PM. For comparison, the bottom figure shows the relative currents measured at the same distance. Fibers illuminated with scintillator light.

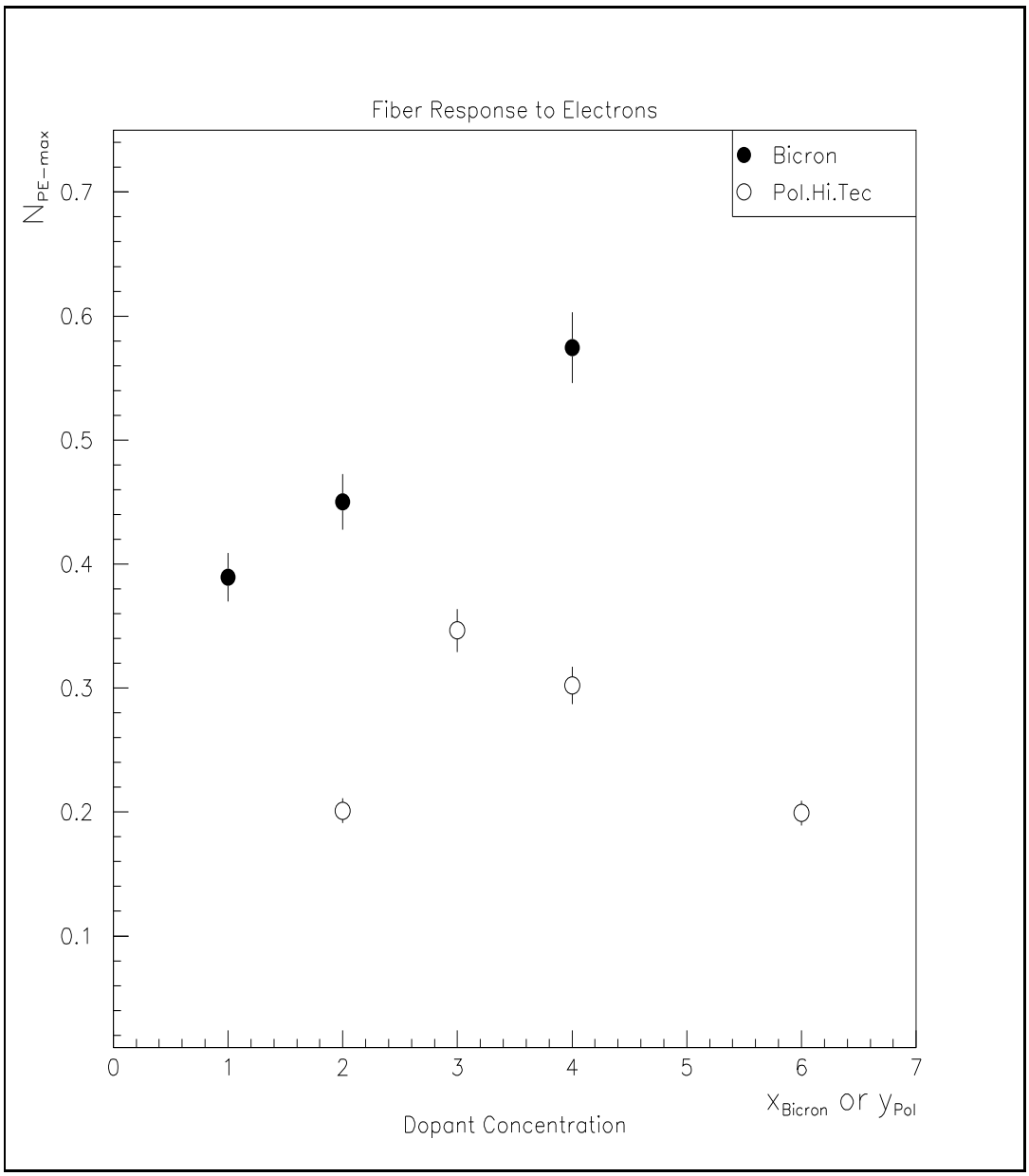

Figure 12: Light output (Cerenkov or scintillating) for fibers with varying concentrations of dopant from Bicron and Pol.Hi.Tech. Peak photolectron yield measured at 50 cm from the PMT is shown.

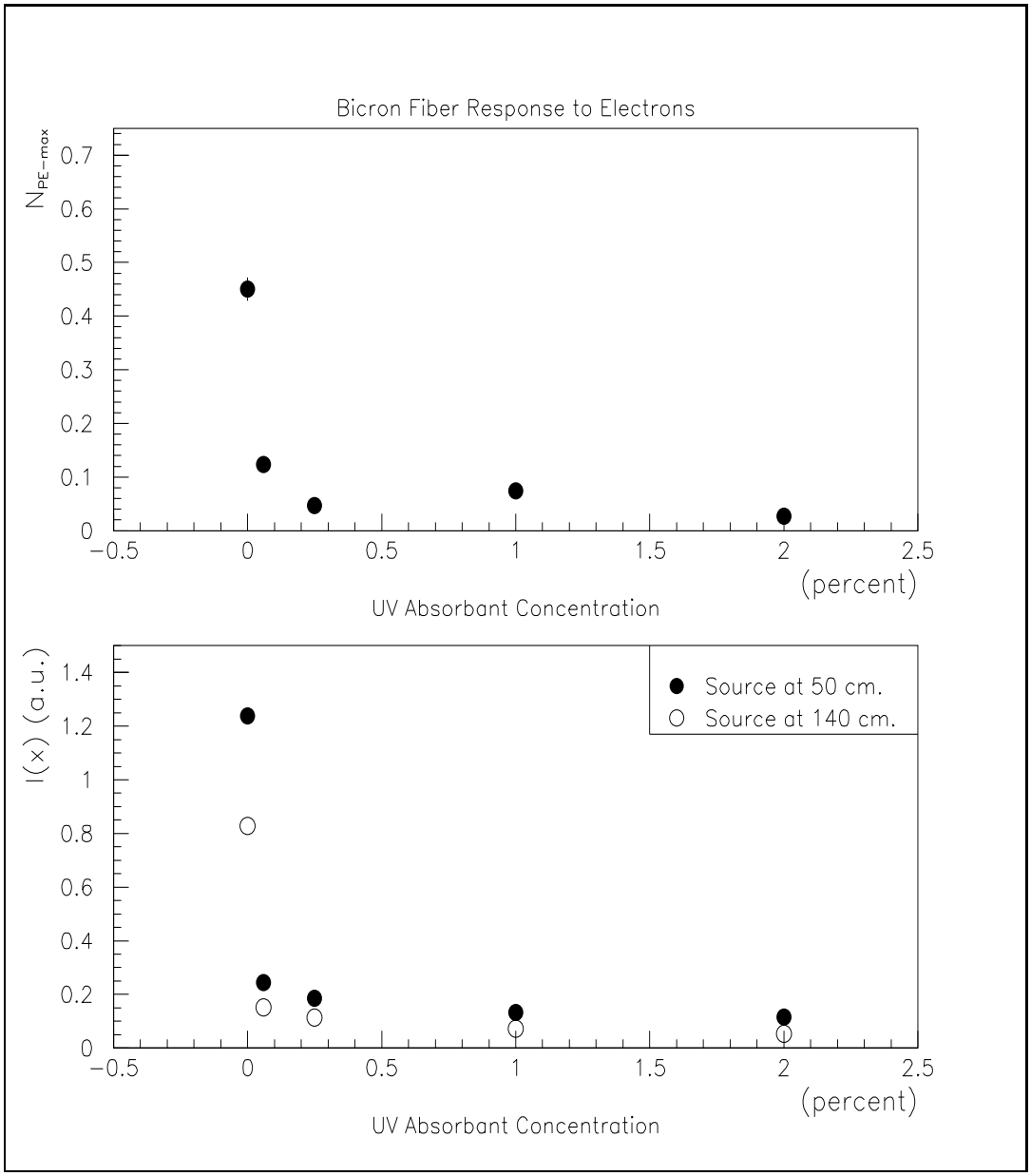

Figure 13: Light output (Cerenkov or scintillating) for fibers with varying concentrations of UVA from Bicron. The top figure shows the peak photolectron yield measured at 50 cm from the PM. For comparison, the bottom figure shows the the relative current measured at 50 and 140 cm.

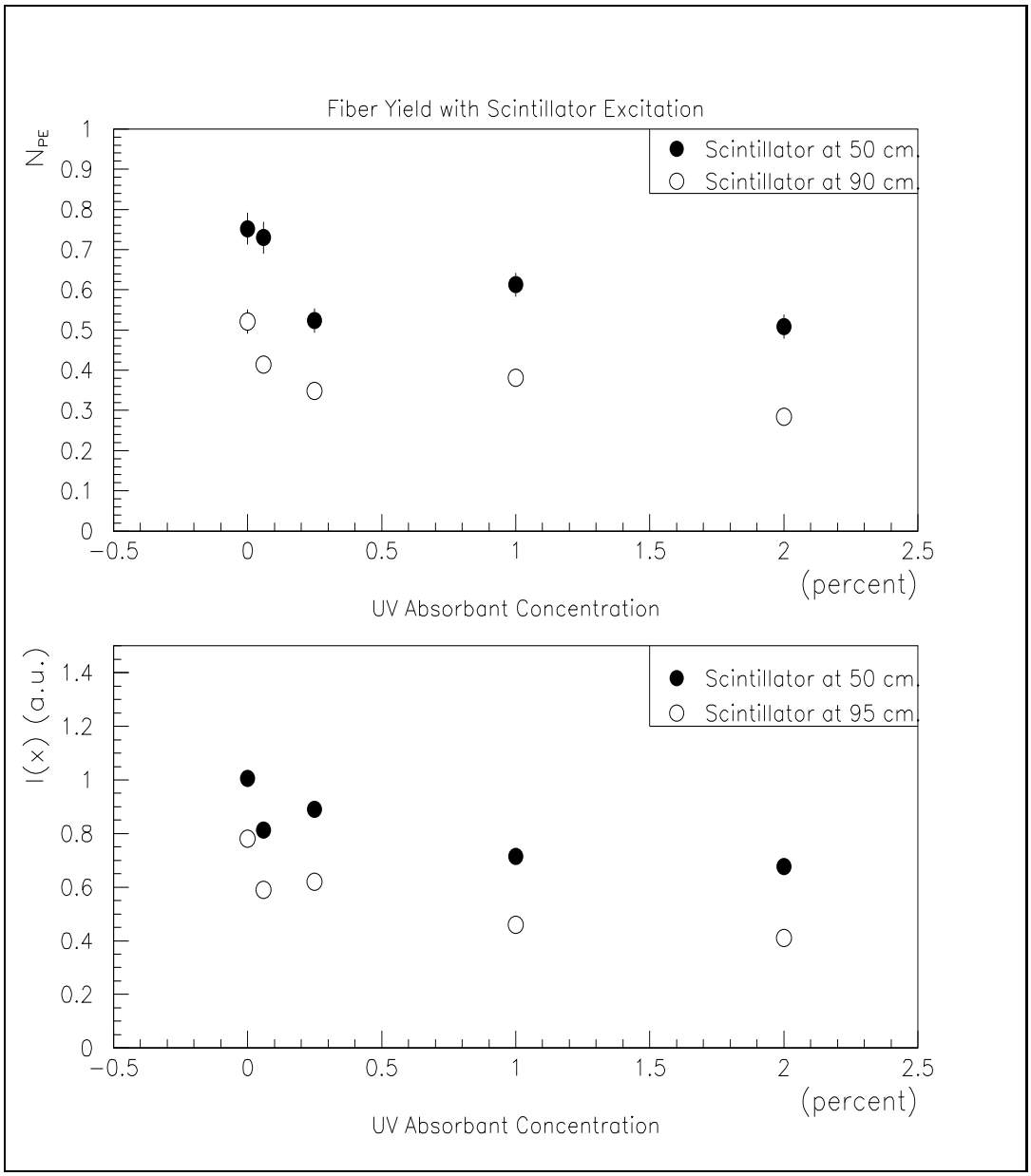

Figure 14: Light yields for BCF99-28 fibers with varying concentrations of UVA. The top figure shows the photolectron yield at 50 and 90 cm from the PMT. For comparison, the bottom figure shows the relative currents. Fibers illuminated with scintillator light.

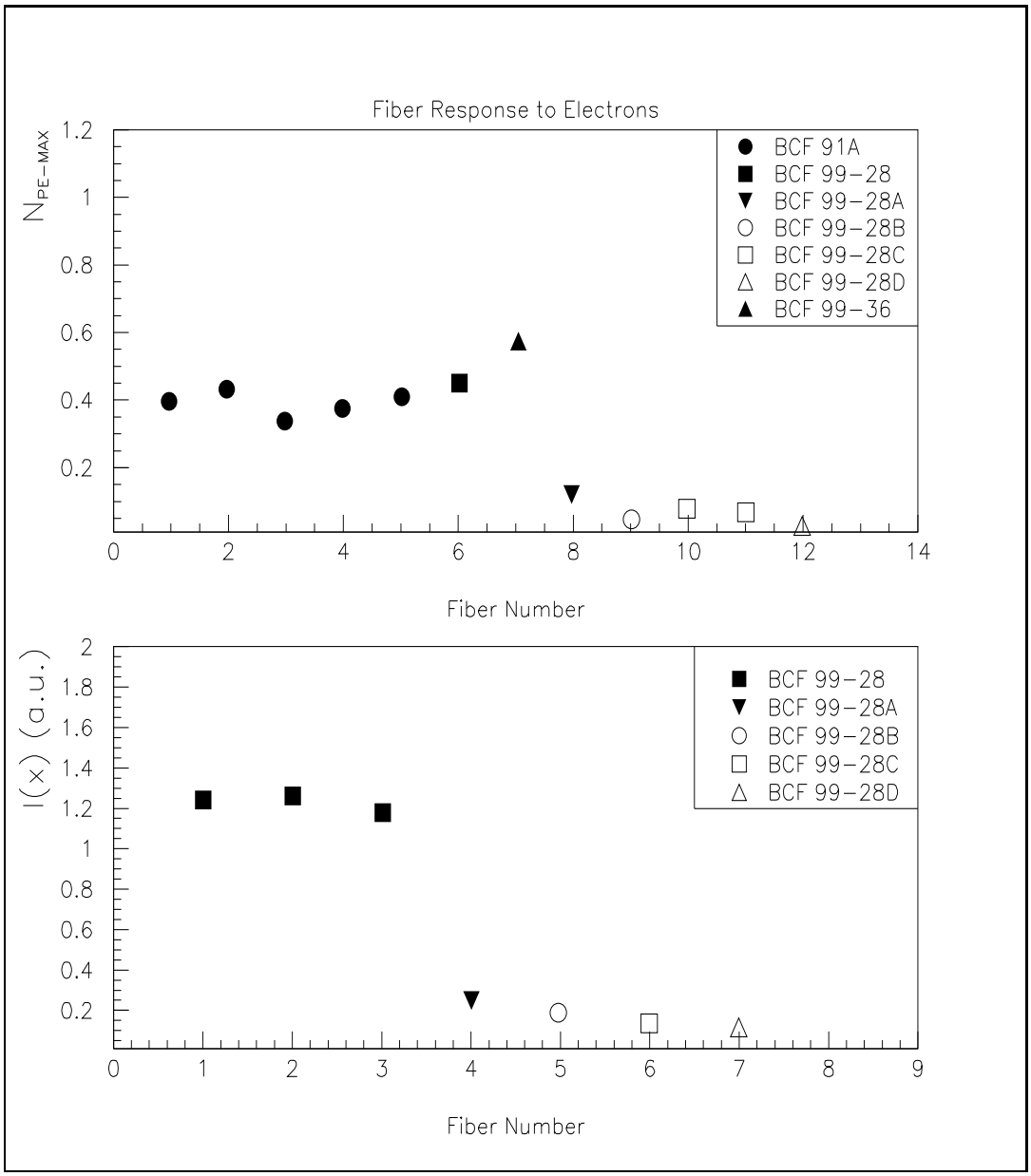

Figure 15: Summary of the light output (Cerenkov or scintillation) for some of the fibers tested (different dopant and UVA concentrations). $N_{pe_{MAX}}$ is the peak of the photoelectron distribution.

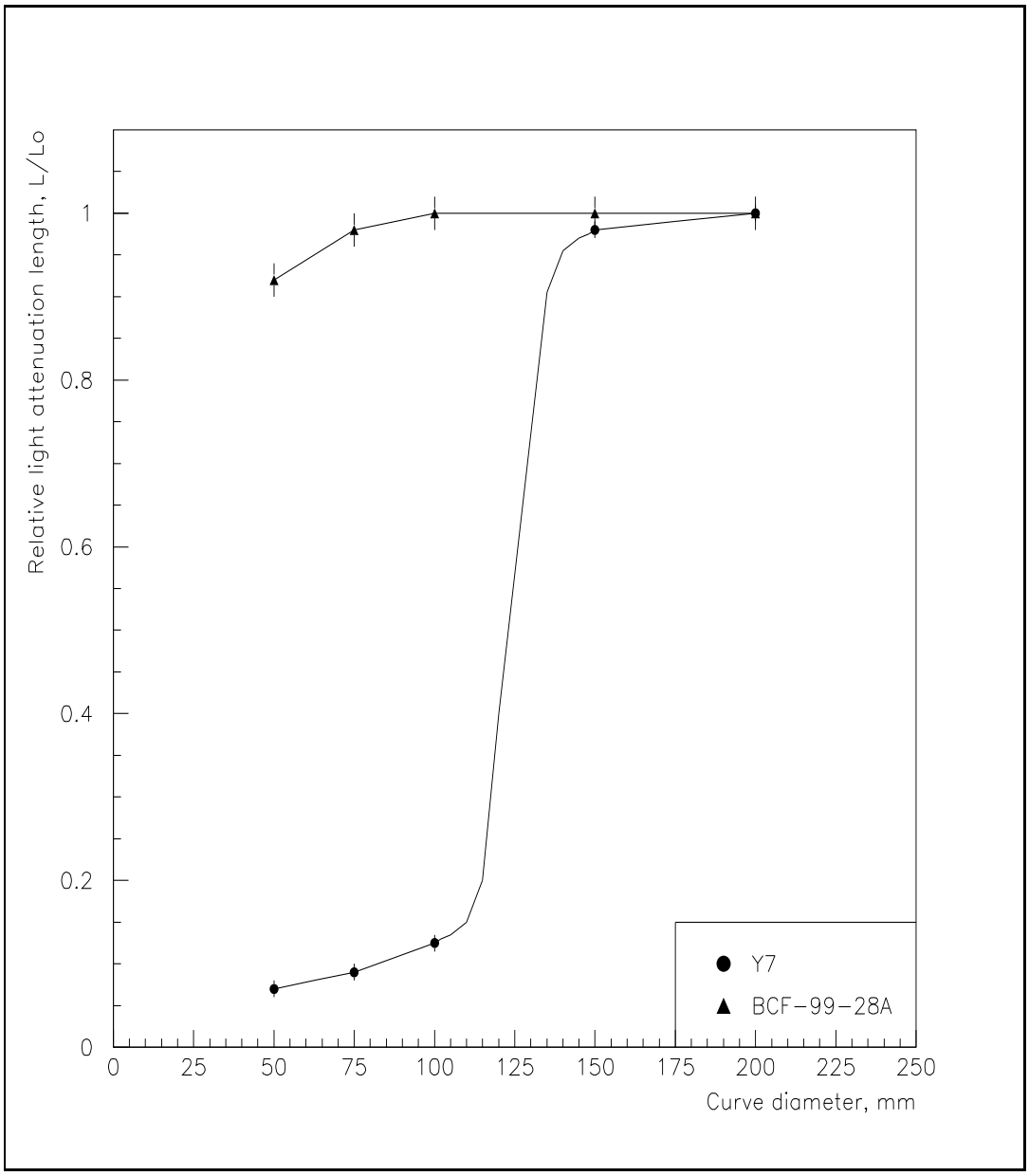

Figure 16: Relative attenuation length as function of curvature radius for BCF99-28A and Y7 fibers. The lines are only to guide the eye.